

Unusual vortex structure in ultrathin Pb (Zr 0.5 Ti 0.5) O 3 films

Zhongqing Wu, Ningdong Huang, Zhirong Liu, Jian Wu, Wenhui Duan, and Bing-Lin Gu

Citation: *Journal of Applied Physics* **101**, 014112 (2007); doi: 10.1063/1.2404534

View online: <http://dx.doi.org/10.1063/1.2404534>

View Table of Contents: <http://scitation.aip.org/content/aip/journal/jap/101/1?ver=pdfcov>

Published by the [AIP Publishing](#)

Articles you may be interested in

[High piezoelectricity of Pb \(Zr , Ti \) O 3 -based ternary compound thin films on silicon substrates](#)

Appl. Phys. Lett. **94**, 122909 (2009); 10.1063/1.3103553

[Multiferroic properties of Ni 0.5 Zn 0.5 Fe 2 O 4 – Pb \(Zr 0.53 Ti 0.47 \) O 3 ceramic composites](#)

J. Appl. Phys. **104**, 104109 (2008); 10.1063/1.3021349

[Stress dependence and scaling of subcoercive field dynamic hysteresis in 0.5 Pb \(Zr 1 / 2 Ti 1 / 2 \) O 3 – 0.5 Pb \(Zn 1 / 3 Nb 2 / 3 \) O 3 ceramic](#)

J. Appl. Phys. **104**, 104103 (2008); 10.1063/1.3021287

[Thickness and coupling effects in bilayered multiferroic CoFe 2 O 4 / Pb \(Zr 0.52 Ti 0.48 \) O 3 thin films](#)

J. Appl. Phys. **103**, 124109 (2008); 10.1063/1.2940014

[Ferroelectricity and local currents in epitaxial 5- and 9 - nm -thick Pb \(Zr , Ti \) O 3 ultrathin films by scanning probe microscopy](#)

Appl. Phys. Lett. **86**, 012903 (2005); 10.1063/1.1843288



Re-register for Table of Content Alerts

Create a profile.



Sign up today!



Unusual vortex structure in ultrathin $\text{Pb}(\text{Zr}_{0.5}\text{Ti}_{0.5})\text{O}_3$ films

Zhongqing Wu, Ningdong Huang, Zhirong Liu, Jian Wu, Wenhui Duan,^{a)} and Bing-Lin Gu

Center for Advanced Study and Department of Physics, Tsinghua University, Beijing 100084, People's Republic of China

(Received 31 May 2006; accepted 22 October 2006; published online 11 January 2007)

Using a first-principles-based approach, we determine the ferroelectric pattern in $\text{PbZr}_{0.5}\text{Ti}_{0.5}\text{O}_3$ ultrathin film. It is found that vortex stripes are formed in the system. The relation between the vortex stripes and the 180° domains is discussed. When a local external field is exerted, the vortex stripe transforms into the vortex loop structure, which leads to the formation of a smaller domain with the polarization antiparallel to the field in the center of the field region. This may provide a convenient way to manipulate nanodomains in thin films. © 2007 American Institute of Physics. [DOI: 10.1063/1.2404534]

I. INTRODUCTION

During the past decade, the extensive research on ferroelectric thin films has been carried out not only due to their promising applications in microelectronics such as nonvolatile random access memories¹⁻³ but also due to their novel physical properties. Ferroelectricity is a collective phenomenon resulting from the delicate balance between the long-range dipole interaction and short-range covalent interaction. In nanostructures such as ultrathin films, both long-range dipole and short-range covalent interactions and their balance are varied in regard to those in the bulk. Therefore, it is commonly believed that the nanostructure will exhibit some physical properties distinctly different from those of bulk materials, e.g., the size effects that the ferroelectricity would disappear below a critical size.⁴⁻⁹ Recently, an unusual atomic off-center displacements vortex pattern in BaTiO_3 nanodot was revealed in simulation.¹⁰ In ferroelectric ultrathin films, the periodic 180° stripe domains have been observed with x-ray study^{5,11} and simulated using a first-principles based approach.^{8,12,13}

Generally, the ferroelectric nanodomain is read or written with a metallic tip of some kinds of microscope such as atomic force microscope. Therefore, it is important to clarify how the ferroelectric pattern of ultrathin films is influenced by the local field produced by the tip. The influence of a uniform external electric field on the domain evolution in ferroelectric ultrathin films has been investigated by Lai *et al.*,¹⁴ while the effect of local electric field was seldom studied. Herein, we conducted a first-principles-based computer simulation to investigate this problem. It is found that a polarization vortex loop is induced under a local external field and the polarizations in the center of the field region are antiparallel with the field. This unusual phenomenon may be helpful in manipulating the nanostructure in the ultrathin film.

II. METHOD

The system we investigated is the disorder $\text{Pb}(\text{Zr}_{0.5}\text{Ti}_{0.5})\text{O}_3$ (PZT) thin films surrounded by vacuum. We adopt the effective Hamiltonian of PZT alloys proposed by Bellaiche, Garcia, and Vanderbilt,¹⁵ which is derived from first-principles calculations, to predict the properties of the system by Monte Carlo simulation. The method can provide the microscopic information about the atomic off-center displacements and therefore is especially suitable for investigating the film without any charge screening. The effective Hamiltonian is represented by a low-order Taylor expansion of the relevant variables (i.e., soft mode and the strain), since the ferroelectric phase transition involves only very small atomic displacements and strain deformations from the high-symmetric cubic structure. For PZT alloys, a compositional degrees of freedom should be included in the effective Hamiltonian. Therefore, the total energy E is written as the sum of an average energy and a local energy^{15,16}

$$E(\{\mathbf{u}_i\}, \{\mathbf{v}_i\}, \eta_H, \{\sigma_j\}) = E_{\text{ave}}(\{\mathbf{u}_i\}, \{\mathbf{v}_i\}, \eta_H) + E_{\text{loc}}(\{\mathbf{u}_i\}, \{\mathbf{v}_i\}, \{\sigma_j\}), \quad (1)$$

where \mathbf{u}_i is the local soft mode in the i th unit cell and associated with the local electrical dipoles $\mathbf{P}_i = Z^* \mathbf{u}_i$ (Z^* is the effective charge of the local mode), \mathbf{v}_i is the dimensionless local displacement,¹⁷ η_H is the homogeneous strain tensors, and $\sigma_j = \pm 1$ represents the presence of a Zr or Ti atom at the j th lattice site of the $\text{Pb}(\text{Zr}_{0.5}\text{Ti}_{0.5})\text{O}_3$. All the parameters of the Hamiltonian are derived from the first principle calculations and are given in Refs. 15 and 16. In our simulations, we do not include the external term of surface effect proposed by Fu and Bellaiche while simulating nanoscopic structures since they have demonstrated that the term has almost no effect on the polarization pattern.^{10,18} The fact that the calculated critical thickness⁸ is well consistent with the x-ray study⁵ further justifies our earlier treatment.

The energy E_{ave} can be obtained by using the virtual crystal approximation (VCA). Within the VCA, a $\text{Pb}\langle B \rangle\text{O}_3$ simple system is created, where the $\langle B \rangle$ atom is a virtual atom involving a kind of potential average between Zr and Ti atoms. The energy E_{loc} is derived by treating the alloy con-

^{a)} Author to whom correspondence should be addressed; electronic mail: dw@phys.tsinghua.edu.cn

figuration $\{\sigma_j\}$ as a perturbation of the VCA system. E_{ave} consists of five parts: a local mode self energy, a dipole-dipole interaction, a short-range interaction between soft modes, an elastic energy, and an interaction between the local modes and local strain. The effective Hamiltonian possesses a comparable accuracy and has been successfully applied to many ferroelectric materials, including a simple BaTiO_3 ,^{10,19} PbTiO_3 ,⁷ and KNbO_3 (Ref. 20) system, and a complex $\text{Pb}(\text{Zr},\text{Ti})\text{O}_3$ (Refs. 15, 21, and 22) and $\text{Pb}(\text{Sc},\text{Nb})\text{O}_3$ (Refs 23–25) solid solution. In particular, the simulation based on the earlier Hamiltonian confirmed the presence of an *A*-type monoclinic phase in the *T*-*x* phase diagram of the disordered $\text{Pb}(\text{Zr}_{1-x}\text{Ti}_x)\text{O}_3$ alloy.¹⁵

We adopt the corrected three-dimensional Ewald method, whose validity has been verified analytically by Bródka and Grzybowski,²⁶ to efficiently calculate the long-range dipole-dipole interaction energy in thin films which lack the periodicity in the out-of-plane direction. In this scheme, a small empty space (about three times of the film thickness) introduced in the simulation box to surround the film can lead to very well converged results. The *z* axis ([001] direction) is taken along the growth direction of the film, and the *x* and *y* axes are chosen to be along the pseudocubic [100] and [010] directions. The influence of the substrate is imposed by confining the homogeneous in-plane compressive strain. Namely, $\eta_1 = \eta_2 = 2\%$ and $\eta_6 = 0$. The temperature of the simulation is 50 K, corresponding to a rescaled experimental temperature of 30 K.¹⁵

III. RESULTS AND DISCUSSION

We first investigate in detail the polarization pattern in the ultrathin film under zero field, which is helpful for clarifying the effect of local electric field. As our previous work demonstrated, the polarization is along the in-plane direction if the thin film is free strain. However, realistic compressive strain from the substrate will suppress the in-plane polarization. Instead the periodic out-of-plane 180° stripe domains appear in the films under 2% compressive strain.⁸ Now we further find that the stripes exhibit unusual microscopic structures. An example of a $15 \times 15 \times 4$ supercell is given in Fig. 1. A unique vortex structure can be clearly observed on the *x*-*z* plane [Fig. 1(a)]. The clockwise and anticlockwise vortex appear alternately. The structure is similar to magnetic closure domain pattern observed in ultrathin film by Dürr *et al.*²⁷ and Neudert *et al.*²⁸ This vortex structure extends along the *y* axis as the vortex stripe. One of the outcomes of the vortex stripe is that the local modes perpendicular to the stripe, u_x , also form the stripe structure in each *x*-*y* plane near film surface [see Fig. 1(b) for *z*=1 plane] and strikingly, align head to head. The 180° out-of-plane polarization stripe domain wall is located at the center of vortex. Therefore, each out-of-plane polarization domain does not superpose with the vortex stripe but strides across two neighboring vortex stripes. The number of unit cells along periodic directions in the earlier example, 15×15 , is just chosen to be approximately two times as the domain width.⁸ Other supercells, such as $20 \times 20 \times 4$ and $20 \times 20 \times 8$, are also used in our simulations, where similar vortex stripe structures are ob-

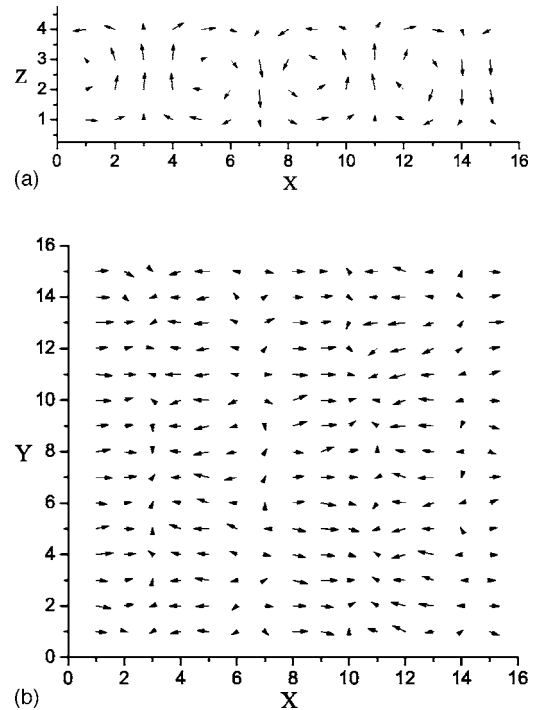


FIG. 1. Local-mode displacement, \mathbf{u}_i , of the cell in (a) the *y*=8 plane and (b) the *z*=1 plane of $15 \times 15 \times 4$ supercell. The arrows give the directions of these displacements, projected on corresponding planes, and the arrow length indicates the projected magnitude.

served. The vortex stripe structure is consistent with the simulation with partial screening by Lai *et al.*¹⁴

The film thickness and the stripe width just denote two characteristic sizes of the vortex. The vortex expands with increasing film thickness and then we can understand intuitively that the period of the stripe domains increases with the film thickness. The other factors, such as the temperature, strain, and concentration inhomogeneities, are found to have little influence on the stripe periods. For example, the disorder PZT and [111] ordered PZT films have the same stripe period. Furthermore, the stripe period is unchanged in morphotropic phase boundary ($0.46 < x < 0.5$, *x* is the Ti concentration) where the parameters of the Hamiltonian are valid. While the film thickness is of four unit cells (1.6 nm), the simulated stripe period is 2.8 nm, which is quantitatively well consistent with the experimental measurement.¹¹

The earlier vortex structure comes from the delicate balance between the long-range dipole interaction and short-range covalent interaction. For the dipole-dipole interaction, the alignment of head to end is favorable in energy, while the head to head is unfavorable. Due to the existence of the vacuum and the absence of the screening effect, the surface dipoles tend to align parallel with the surface to stabilize the dipole-dipole interaction. The short-range covalent interaction supports the dipoles to change smoothly. In the internal layers, because of the large compressive strain, the local mode tends to align along the direction normal to the film. The vortex structure meets all the earlier demands, and with periodical arrangement, effectively eliminates the depolarization field.

Now we turn our attention to the influence of the local field on the microscopic structure. In our simulation, the lo-

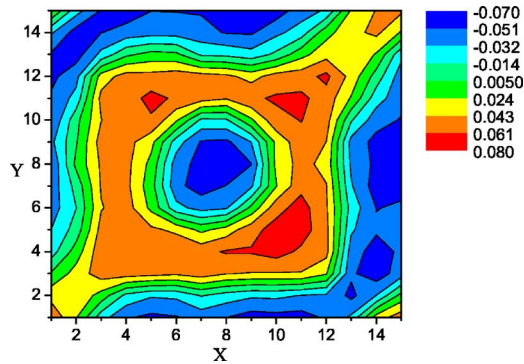


FIG. 2. (Color online) The out-of-plane local modes of a $15 \times 15 \times 4$ supercell. A local field $E=2 \times 10^7$ V/m is exerted on a smaller region of $10 \times 10 \times 4$ (namely $N_E=10$).

cal field produced by the tip is assumed to be exerted in a smaller region, $N_E \times N_E \times 4$, of the supercell. The electric field is homogeneous inside the exerted region. Due to the periodic boundary condition adopted in the film plane, the local field will appear periodically, which is similar to a field created by the array of the tips. Generally, we can expect that a ferroelectric nanodomain will be formed when a local field is exerted. However, to our surprise, the actual situation is not so simple. Figure 2 depicts the out-of-plane local mode (namely polarization) of the film with $E=2 \times 10^7$ V/m and $N_E=10$. Although the field aligns most out-of-plane polarizations in the field region along the field direction, the polarizations near the center of the field region are antiparallel with the field. The smaller region (nanodomain) where the out-of-plane polarizations are antiparallel with the field is approximately round in shape. Furthermore, interestingly, the average magnitude of out-of-plane polarization in this nanodomain are little larger than that of stripe domain in absence of field, which respectively are 0.0396 and 0.0387 a.u. With increasing field strength, the size of nanodomain decreases, but its average magnitude of out-plane polarization is almost unchanged.

More details of the polarization pattern are given in Fig. 3. Although the clockwise and anticlockwise vortexes still appear alternately in the x - z plane [Fig. 3(a)], the straight stripes in the x - y plane are destroyed by the local field and a vortex loop appears in the field region as shown in Fig. 3(b). Our detailed analysis shows that the vortex loop structure could be regarded as being formed by the rotation of the inner vortex around the oo' axis [Fig. 3(a)]. Figure 3(b) supports this conclusion, showing that the boundary line between the inner vortex and the outer vortex is roughly round (the dashed circle in the graphics) and the local modes inside the circle are almost radialized. Similar proof can also be observed in Fig. 2. Therefore, our simulations demonstrate that the local field can result in the transformation from the vortex straight stripe into the vortex loop and form a nanodomain. Lai *et al.*¹⁴ reported the formation of a nanobubble on the ferroelectric film under a uniform external field. Although in our case the area where the field is applied is larger than half of the simulation cell, the situation is essentially different from that under a uniform field. The key point is that there are some areas where no field is applied, thus the

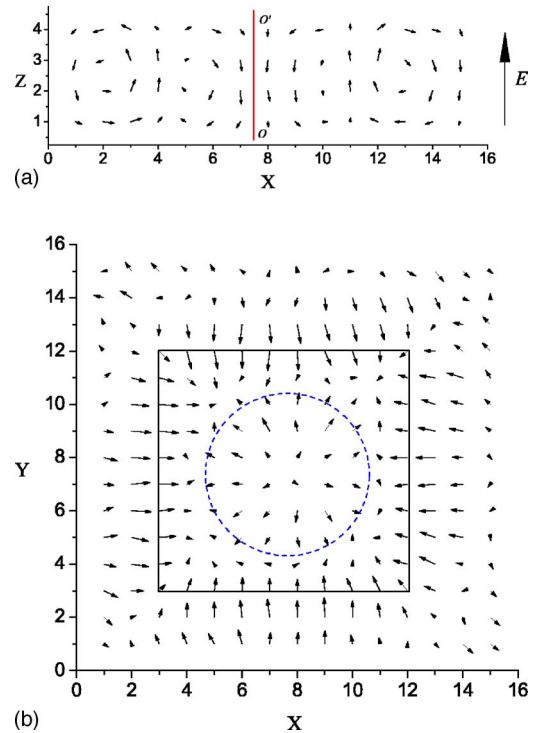


FIG. 3. (Color online) Local-mode displacements, \mathbf{u}_i , of the cell in (a) the $y=8$ plane and (b) the $z=1$ plane of a $15 \times 15 \times 4$ supercell. The arrows give the directions of these displacements, projected on corresponding planes, and the arrow length indicates the projected magnitude. A local field $E=2 \times 10^7$ V/m along the z axis is exerted on a smaller region $10 \times 10 \times 4$ denoted by the solid line. The dashed line shows the boundary of the inner vortex and the outer vortex.

domain structure can be optimized by arranging more parallel (to the applied field) domains into the area with a field and more antiparallel domains into the area without a field to lower the total energy (see the following), which is impossible in the case under a uniform field. This is the reason why the vortex loop is induced by a smaller field (less than 2×10^7 V/m) in our case, while a much higher field (about 20×10^7 V/m) is required to induce the nanobubble in the uniform case. It also results in the consequence that the vortex loop is circular in shape in our case while the nanobubble is elongated in the uniform case.

The earlier unusual phenomena are closely related with the character of the stripe. On the one hand, the shape of vortex is rather stable. The stripe width is determined only by the film thickness and is almost independent of the temperature and compressive strain until the stripe disappears. The influence of the global external field (i.e., the field is exerted on the whole supercell) on the stripe width is also considerably small. Our simulations indicate that the stripe width does not alter appreciably after applying a very large external field (10^8 V/m) to the supercell. All of these results clearly demonstrate that the shape of vortex is very stable. On the other hand, the stripe structure composed of the vortexes is considerably flexible. Our simulations show that besides the straight stripe mentioned earlier, many kinds of bent stripes also correspond to local minimum of the energy. Although the internal energy of these bent stripes is larger than that of the straight stripe, the energy difference is very

small. Therefore, we can conveniently trap some bent stripes by applying and removing the local field with a different configuration. For example, a vortex loop structure similar to that shown in Fig. 2 can be trapped by applying and then removing the local field. The corresponding internal energy is larger than that of the straight stripe by only about $1 \text{ meV}/5 \text{ atoms}$. The diameter of the inner domain in the vortex loop structure is smaller than the stripe period τ ($\tau \approx 7$ in the current case). Therefore, when N_E (denoting the field region of the external local field) exceeds τ , no configuration of polarizations can make the whole field region occupied by the parallel phase. Alternately, a loop structure with antiparallel polarization in the center, as those in Figs. 2 and 3, is the optimum scheme to have as much parallel polarization as possible in the action range of the local field. This is the reason of the appearance of the central antiparallel domain. When N_E (the external field range) further increases, the number of the loop stripe in the structure will increase due to the fact that the width of the loop stripe is almost fixed, and a parallel domain (data not shown) may appear in the center.

Our simulations indicate that the same phenomena also appear in thicker ultrathin films (such as the films with the thickness of six and eight unit cells). Furthermore, although the radius of the central antiparallel domain decrease with the field strength increase, its maximum is only determined by the film thickness. The influence of the size of the field region and the in-plane size of the supercell on the radius of the antiparallel domain could be overlooked. The maximum of radius of the antiparallel domain is a little larger than half of the stripe width and is much smaller than the size of the field region (denoted by N_E). Therefore, our results imply that we can write a nanodomain whose size is far smaller than the radius of the tip. This unique character may have the potential application in improving the storage densities of ferroelectric memory. In general, in order to improve the storage density we need to decrease the radius of the tip since the size of tip is a very important factor to determine the lower limits of the radius of nanodomain. However, it is obvious that decreasing of the tip radius has its own limit below which it would be very difficult to further reduce the tip. Our simulation suggests a possible approach to break through the limit imposed by the radius of the tip. According to our calculated results and the fact that the stripe width of the 100-nm-thick PbTiO_3 film is about 10 nm by x-ray study,¹¹ we can estimate that the radius of the antiparallel domain in a 100-nm-thick PbTiO_3 film is about 5 nm, corresponding to a considerably small dot.

It should be noted that the formation of the vortex structures such as the vortex stripe and loop is closely related with the electric boundary condition adopted in our simulations (i.e., no surface charge induced by polarization is screened). With enhancing the screening of the surface charges, the vortex stripe domains will transform into a monodomain.¹² However, the perfect screening is not achieved even under short circuit boundary conditions in ultrathin film. For example, a sizable depolarization field was quantified by Junquera and Ghosez⁹ through a first principles calculation. Such a field was recently suggested to explain the experimental changes of the coercive fields with the film

thickness.²⁹ The effect of the screening becomes weaker when the top electrode is replaced by the metallic tip, which is just the case in writing the nanodomain in ferroelectric films. A larger depolarization field will be formed in those ferroelectric films. Furthermore, the vortex polarization pattern is very stable against the electric field. Our simulation showed that the vortex pattern persists until the electric field is so high that the film becomes a monodomain. Therefore, the phenomenon that the direction of the polarization is antiparallel with the field near the center of the field region will be promisingly observed in perovskite ferroelectric film.

Similar antiparallel poling reversal phenomenon has been reported by Abplanalp *et al.*³⁰ and Morita *et al.*³¹ However, this phenomenon is not induced by the depolarization field and has a different microscopic origin from ours. In Abplanalp *et al.*'s study,³⁰ the antiparallel reversal corresponds to ferroelastoelectric switching and is achieved in BaTiO_3 thin film by simultaneously applying electric field and compressive stress with the tip of a scanning force microscope. In Morita *et al.*'s study,³¹ the depolarization field should be small since the film can be poled into a monodomain. Although the reason of antiparallel poling reversal is still unclear, it is suggested that this phenomenon is related to the mechanical force imposed by the tip. Furthermore, the antiparallel poling appears only after the electric field is removed, which is different from our results in that the antiparallel polarization starts to appear under the local field.

IV. CONCLUSION

In summary, the ferroelectricity of ultrathin PZT films without any charge screening has been investigated with the Monte Carlo simulations based on a first-principles-derived Hamiltonian. The off-center displacements in the films of several unit cells exhibit vortex stripes with unusual characters. On the one hand, the shape of the vortex is rather stable. On the other hand, the stripe structure composed of the vortex is considerably flexible and can be easily manipulated. The unusual characters of the vortex stripe lead to an interesting phenomenon: the local field can transform the vortex straight stripe into the vortex loop structure, which results in the formation of a round-shape domain with the polarization antiparallel with the field near the center of the field region. The area of the antiparallel domain is much smaller than the area of the field region. This implies a way to write a very small nanodomain with the general tip, which might have some potential application in improving the storage densities of ferroelectric memory.

ACKNOWLEDGMENTS

This work was supported by State Key Program of Basic Research Development of China (Grant No. 2006CB605105), the National Natural Science Foundation of China (Grant Nos. 10325415 and 50432030), and Ministry of Education of China.

¹J. F. Scott and C. A. Araujo, *Science* **246**, 1400 (1989).

²R. Waser and A. Rüdiger, *Nat. Mater.* **3**, 81 (2004).

³C. H. Ahn, K. M. Rabe, and J.-M. Triscone, *Science* **303**, 488 (2004).

⁴A. V. Bune, V. M. Fridkin, S. Ducharme, L. M. Blinov, S. P. Palto, A. V.

- Sorokin, S. G. Yudin, and A. Zlatkin, *Nature (London)* **391**, 874 (1998).
- ⁵D. D. Fong, G. B. Stephenson, S. K. Streiffer, J. A. Eastman, O. Auciello, P. H. Fuoss, and C. Thompson, *Science* **304**, 1650 (2004).
- ⁶Y. G. Wang, W. L. Zhong, and P. L. Zhang, *Phys. Rev. B* **51**, 5311 (1995).
- ⁷P. Ghosez and K. M. Rabe, *Appl. Phys. Lett.* **76**, 2767 (2000).
- ⁸Z. Q. Wu, N. D. Huang, Z. R. Liu, J. Wu, W. H. Duan, B. L. Gu, and X. W. Zhang, *Phys. Rev. B* **70**, 104108 (2004).
- ⁹J. Junquera and P. Ghosez, *Nature (London)* **422**, 506 (2003).
- ¹⁰H. Fu and L. Bellaiche, *Phys. Rev. Lett.* **91**, 257601 (2003).
- ¹¹S. K. Streiffer, J. A. Eastman, D. D. Fong, C. Thompson, A. Munkholm, M. V. R. Murty, O. Auciello, G. R. Bai, and G. B. Stephenson, *Phys. Rev. Lett.* **89**, 067601 (2002).
- ¹²I. Kornev, H. Fu, and L. Bellaiche, *Phys. Rev. Lett.* **93**, 196104 (2004).
- ¹³S. Tinte and M. G. Stachiotti, *Phys. Rev. B* **64**, 235403 (2001).
- ¹⁴B.-K. Lai, I. Ponomareva, I. I. Naumov, I. Kornev, H. Fu, L. Bellaiche, and G. J. Salamo, *Phys. Rev. Lett.* **96**, 137602 (2006).
- ¹⁵L. Bellaiche, A. Garcia, and D. Vanderbilt, *Phys. Rev. Lett.* **84**, 5427 (2000).
- ¹⁶L. Bellaiche, A. Garcia, and D. Vanderbilt, *Ferroelectrics* **266**, 41 (2002).
- ¹⁷W. Zhong, D. Vanderbilt, and K. M. Rabe, *Phys. Rev. Lett.* **73**, 1861 (1994); *Phys. Rev. B* **52**, 6301 (1995).
- ¹⁸Although the earlier effective Hamiltonian was developed for bulk PZT, the surface effect is partially and implicitly considered during the simulations on the films by (i) including the effect of the broken bonds in the surfaces, which is substantial for the surface energy; and by (ii) relaxing the local soft mode vectors and inhomogeneous strain, which partially reflects the effect of surface relaxation.
- ¹⁹J. Íñiguez and D. Vanderbilt, *Phys. Rev. Lett.* **89**, 115503 (2002).
- ²⁰H. Krakauer, R. Yu, C. Z. Wang, and C. Lasota, *Ferroelectrics* **206**, 133 (1998).
- ²¹N. Huang, Z. Liu, Z. Wu, J. Wu, W. Duan, B. L. Gu, and X. W. Zhang, *Phys. Rev. Lett.* **91**, 067602 (2003).
- ²²I. A. Kornev and L. Bellaiche, *Phys. Rev. Lett.* **91**, 116103 (2003).
- ²³R. Hemphill, L. Bellaiche, A. Garcia, and D. Vanderbilt, *Appl. Phys. Lett.* **77**, 3642 (2000).
- ²⁴A. M. George, J. Íñiguez, and L. Bellaiche, *Nature (London)* **413**, 54 (2001).
- ²⁵J. Íñiguez and L. Bellaiche, *Phys. Rev. Lett.* **87**, 095503 (2001).
- ²⁶A. Bródka and A. Grzybowski, *J. Chem. Phys.* **117**, 8208 (2002).
- ²⁷H. A. Dürr, E. Dudzik, S. S. Dhesi, J. B. Godekoop, G. van der Laan, M. Belakhovsky, C. Mocuta, A. Marty, Y. Samson, *Science* **284**, 2166 (1999).
- ²⁸A. Neudert, J. McCord, D. Chumakov, R. Schäfer, and L. Schultz, *Phys. Rev. B* **71**, 134405 (2005).
- ²⁹M. Dawber, P. Chandra, P. B. Littlewood, and J. F. Scott, *J. Phys.: Condens. Matter* **15**, L393 (2003).
- ³⁰M. Abplanalp, J. Fousek, and P. Günter, *Phys. Rev. Lett.* **86**, 5799 (2001).
- ³¹T. Morita and Y. Cho, *Appl. Phys. Lett.* **84**, 257 (2004).